

# Dumb Holes and the Effects of High Frequencies on Black Hole Evaporation

W. G. Unruh  
*CIAR Cosmology Program*  
*Dept. of Physics*  
*University of B. C.*  
*Vancouver, Canada V6T 1Z1*  
*email: unruh@physics.ubc.ca*

## Abstract

The naive calculation of black hole evaporation makes the thermal emission depend on the arbitrary high frequency behaviour of the theory where the theory is certainly wrong. Using the sonic analog to black holes—dumb holes— I show numerically that a change in the dispersion relation at high frequencies does not seem to alter the evaporation process, lending weight to the reality of the black hole evaporation process. I also suggest a reason for the insensitivity of the process to high frequency regime.

## I. DUMB HOLES

Black hole evaporation [1] was one of the most surprising predictions of the field of quantum field theory in curved backgrounds. Since the phenomenon has not been observed experimentally, it is of crucial importance that the assumptions underlying the prediction be examined especially carefully so as to try to understand the process as deeply as possible.

One of the most unsettling features of the derivation is the dependence of the derivation on the behaviour of the fields at arbitrarily high frequencies. In fact, if we trace, in the usual derivation, the origin of the thermal emission from a solar mass sized black hole a second after the formation of the black hole, that thermal radiation has its origin in frequencies in the incoming (vacuum) radiation of the order of  $e^{10^4}$  (where any units make only trivial changes in the exponent). Since  $\hbar\omega$  for such frequencies correspond to masses vastly larger than the mass of the universe, it seems certain that the quantum gravitational effects of such frequencies would completely alter the behaviour of the field at such scales. Would such quantum gravitational effects also destroy the thermal emission from the black hole?

Since we have no quantum theory of gravity, this question is difficult to answer. However, the thermal emission is not only characteristic of black holes, it is also characteristic of dumb holes, the sonic analog of black holes [2] [3]. A dumb hole forms when the velocity of the fluid exceeds the velocity of sound at some closed surface. That surface forms a sonic horizon, an

exact sonic analog of a black hole horizon. As I showed in 1981, the propagation of sound waves in such a hypersonic fluid flow are exactly the same as the propagation of scalar waves in a black hole spacetime.

Since the derivation is not commonly known, it worthwhile repeating it here. The isentropic equation for fluid flow in a medium which is has an equation of state  $p = p(\rho)$  is given by

$$\begin{aligned}\rho(\dot{\mathbf{v}} + \mathbf{v} \cdot \nabla \mathbf{v}) &= -\nabla p(\rho) \\ \dot{\rho} + \nabla(\rho \mathbf{v}) &= 0\end{aligned}\tag{1}$$

I will assume that the flow is irrotational, so that we can write

$$\mathbf{v} = \nabla \Phi\tag{2}$$

The first equation can then be written as

$$\nabla \left( \dot{\Phi} + \frac{1}{2} \mathbf{v} \cdot \mathbf{v} + h(\rho) \right) = 0\tag{3}$$

where  $h(\rho) = \int \frac{dp}{\rho}$ , from which we get Bernoulli's equation

$$\dot{\Phi} + \frac{1}{2} \mathbf{v} \cdot \mathbf{v} + h(\rho) = 0\tag{4}$$

(The time dependent constant of integration can be absorbed into  $\Phi$ ). We now introduce the small perturbations of  $\Phi$  and  $\rho$  about the background flow, defining  $\phi = \delta\Phi$  and  $\psi = \frac{\delta\rho}{\rho}$ . We get the equations

$$\begin{aligned}\dot{\phi} + \mathbf{v} \cdot \nabla \phi + c^2 \psi &= 0 \\ \dot{\psi} + \mathbf{v} \cdot \nabla \psi + \nabla^2 \phi + \nabla \ln(\rho) \cdot \nabla \phi &= 0\end{aligned}\tag{5}$$

where  $c^2 = \rho \frac{dh}{d\rho} = \frac{dp}{d\rho}$ . Dividing the first equation by  $c^2$  and adding taking the derivative with respect to  $\frac{d}{dt} + \mathbf{v} \cdot \nabla + \nabla \cdot \mathbf{v}$  we finally obtain

$$\frac{1}{\rho} \left( \frac{d}{dt} + \mathbf{v} \cdot \nabla + \nabla \cdot \mathbf{v} \right) \frac{\rho}{c^2} \left( \frac{d}{dt} + \mathbf{v} \cdot \nabla \right) \phi - \frac{1}{\rho} \nabla \cdot \rho \nabla \phi = 0\tag{6}$$

Now, this is exactly the equation of motion for a scalar wave in the metric

$$\sqrt{(-g)} g^{\mu\nu} = \rho \begin{pmatrix} c^{-2} & \frac{v^i}{c^2} \\ \frac{v^j}{c^2} & \frac{v^i v^j}{c^2} - \delta^{ij} \end{pmatrix}$$

or in four dimensions

$$g_{\mu\nu} = \rho \begin{pmatrix} c^2 - v^2 & v^i \\ v^j & -\delta_{ij} \end{pmatrix}$$

If the flow is stationary, we can define the Killing vector

$$\zeta^\mu = \delta_0^\mu\tag{7}$$

and find the Killing Horizon at the point where  $c^2 = v^2$ . If  $\frac{v^i}{(c^2-v^2)}$  is an integrable vector, we can also define  $d\tau = (dt + \frac{v^i}{(c^2-v^2)}dx^i)$  and get the metric

$$ds^2 = \rho((c^2 - v^2)d\tau^2 - (\delta_{ij} + \frac{v^i v^j}{c^2 - v^2})dx^i dx^j) \quad (8)$$

If we furthermore assume that the flow is radial, ( in which case  $\frac{v^i}{(c^2-v^2)}$  is always integrable) the metric becomes

$$ds^2 = \rho \left( (c^2 - v^2)d\tau^2 - \frac{1}{1 - \frac{v^2}{c^2}}dr^2 - r^2 d\Omega^2 \right)$$

where  $d\Omega^2 = d\theta^2 + \sin^2\theta d\phi^2$  the usual angular metric.

By exactly the same arguments as for black holes, one expects that this hypersonic flow will produce thermal radiation with a temperature given by the ‘‘surface gravity’’ at the black hole horizon, which in this case, results in a temperature

$$T = \frac{1}{2\pi} \frac{dv}{dr} \Big|_{v=c} \quad (9)$$

However this prediction is again made on the assumption that these sonic equations are valid for arbitrarily short wavelengths, a clearly ridiculous assumption. At wavelengths shorter than of order the intermolecular spacing, the equations for sound waves deviate significantly from the low frequency continuum fluid approximation. Does this change in the fluid equations at high frequency alter the prediction of thermal emission? If it does, one begins to loose faith in the black hole predictions. If it does not, perhaps it will give us a clue as to the real origin of the radiation.

While an exact solution of the fluid equations which fully took into account the atomic nature of the fluid would be most welcome, I am unable to supply it. However one of the most significant of the deviations from continuum fluid flow is the change in the dispersion relation for sound waves. Typically at wavelengths approaching the inter atomic spacing, the group velocity of the sound waves drops to values much less than the low frequency value. Can this change in the dispersion relation change the prediction of a thermal spectrum of sound waves emitted from such a dumb hole?

Thus the model I want to test is a model for sound waves within a fluid flow with a sonic horizon, or for scalar waves in a background metric, in which the dispersion relation at high frequencies differs from the usual low frequency form. In particular the model will contain a high frequency cut off, i.e., a frequency above which there are no normal modes for the propagation of sound waves. As Jacobson has argued, a naive cutoff leads to not only a suppression of the thermal emission, but also a suppression of all waves and vacuum fluctuations from the hole. In our model however the cutoff is to arise naturally in the theory.

Because I am interested in the effects of changes at high frequencies to the thermal emission, not in the detailed behaviour of a real fluid, I will simplify the model so as to make the solution as easy as possible while still retaining the features responsible for the thermal emission in the naive theory. Thus, to make the calculations easy, I will look at

a two dimensional model (i.e., one space and one time) of the propagation of waves in a flowing medium and one in which the high frequency dispersion relation is non-standard. I will also assume a constant velocity of sound ( $c=1$ ), and I will assume that the background density  $\rho$  is a constant. (Note that although a two dimensional background flow cannot have a constant density and a varying velocity, this assumption does not change the location of the horizon, nor does it significantly alter the propagation equation of sound waves except at the very lowest frequencies.) The model equation of motion of the scalar waves I will use in examining the effects of alteration of the high frequency behaviour of the theory is

$$(\partial_t + \partial_x v)(\partial_t + v\partial_x)\phi - F^2(\partial_x)\phi = 0 \quad (10)$$

where the function  $F(\kappa)$  is such that  $F$  is an odd analytic function of  $k$ ,  $F(\kappa) = \kappa$  for small  $\kappa$  and  $F(\kappa) = Const$  for large  $\kappa$ . I.e., the dispersion function for the fluid ( taking  $v=0$ ) is

$$\omega^2 = F^2(k)$$

Note that if  $F(\kappa) = \kappa$  for all  $\kappa$ , then we have the simple equation

$$[(\partial_t + \partial_x v)(\partial_t + v\partial_x) - \partial_x^2]\phi = 0 \quad (11)$$

for which we can make the change of variables  $\tau = t + \int \frac{v dx}{(1-v^2)}$  to get

$$\left[ (1-v^2)\partial_\tau^2 - \frac{1}{1-v^2}\partial_x^2 \right] \phi = 0 \quad (12)$$

which has as solution

$$\phi(\tau, x) = f(\tau - z) + g(\tau + z) \quad (13)$$

where  $z = \int \frac{dx}{1-v^2}$ . This is just the equation for a scalar field in a two dimensional black hole spacetime, where near the horizon, we can write

$$ds^2 = 2 \frac{dv}{dx} \Big|_{v=1} (x - x_0) d\tau^2 - \frac{dx^2}{2 \frac{dv}{dx} \Big|_{v=1} (x - x_0)} \quad (14)$$

Just as for the black hole spacetime this leads to the conclusion that the temperature of the emitted radiation is given by

$$T = \frac{1}{2\pi} \frac{dv}{dx} \Big|_{v=1} \quad (15)$$

Alternatively, one can use the analytic continuation arguments to imaginary  $\tau$  time and demand regularity of the Green's function at the horizon in the regular Euclidean metric

$$ds^2 = (1-v^2)d\mathcal{T}^2 + \frac{1}{1-v^2}dx^2 \quad (16)$$

with the identification

$$\frac{dv}{dx}\mathcal{T} + 2\pi = \frac{dv}{dx}T \quad (17)$$

to arrive at the same conclusion.

However, as soon as we alter the dispersion function  $F$ , this analyticity argument fails. Under the analytic continuation of  $\tau = i\mathcal{T}$ , the equation of motion for the field becomes complex, rather than real. One can draw no conclusion from the behaviour of the Green's function for this complex metric, nor does one have any reason to demand that one make the identification of the Euclidean  $\mathcal{T}$  coordinate of eqn. 17, since the equation of motion no longer has a metric that this identification makes regular.

## II. NUMERICAL SOLUTION

In order to determine the consequence to the thermal emission process of the altered dispersion relation, we must go back to basic principles and calculate the Bogoliubov coefficients for the conversion of ingoing positive frequency modes to outgoing negative frequency modes. I have carried out this calculation numerically for a couple of dispersion functions  $F$ .

As is usual, the particle production rate is equal to the overlap integral between a negative frequency final mode and a positive frequency initial mode. One can either start with a positive frequency initial mode, propagate this through the region containing the black or dumb hole, and calculate the negative frequency component of the final mode, or start with a negative frequency final mode and calculate the positive frequency initial component of this by propagation backwards in time. It turns out that the latter is the easier to do numerically. Thus I start with some outgoing purely negative frequency wave packet. I then propagate it backwards in time toward the horizon until it is converted to an initial pulse, and calculate the positive frequency component of that initial packet.

It is here necessary to state, in the case of the non-trivial dispersion relation, what I mean by positive and negative frequency. This is important because the dispersion relation implies that the notion of positive frequency does not refer to positive or negative sign of the frequencies *per se*. The dispersion relation for constant velocity of fluid flow looks like

$$\omega_{\pm} = vk \pm |F(k)| \quad (18)$$

Even if  $v$  is less than unity, there are values of positive  $k$  for which  $\omega_{\pm}$  both are positive, and values of negative  $k$  for which both are positive. In particular if  $k > k_c$ , where  $k_c$  is the solution to  $F(k_c) = vk_c$ , then both possible values,  $\omega_{\pm}$ , are positive. ( $k_c$  represents the wave vector at which the phase velocity of the wave is zero.) Thus, in the sense of the sign of  $\omega$ , there are no positive frequencies at all for  $k > k_c$  and no negative frequencies at all for  $k < -k_c$ . However, the term 'positive frequencies' or 'negative frequencies' refers not to the sign of  $\omega$  (although there is a correlation for free fields) but to fixed frequency modes which have positive or negative norm.

The field equations for the simplified two dimensional model for sound waves (with constant density) can be derived from the action

$$I = \frac{1}{2} \int |\partial_t \phi + v(t, x) \partial_x \phi|^2 - |(F(\partial_x) \phi)|^2 dx \quad (19)$$

which leads to a momentum

$$\pi(t, x) = \partial_t \phi + v(t, x) \partial_x \phi \quad (20)$$

and an inner product

$$\langle \phi, \phi' \rangle = -\frac{i}{2} \int (\phi^*(t, x) \pi'(t, x) - \pi^*(t, x) \phi'(t, x)) dx \quad (21)$$

If we assume a solution with a definite frequency and wave number  $\phi_{\omega, k}(t, x) = \tilde{\phi}(\omega, k) e^{i\omega t + kx}$  and with constant  $v$ , we find that

$$\langle \phi_{\omega, k}(t, x), \phi_{\omega, k}(t, x) \rangle = \pm F(k) \int |\phi_{\omega, k}|^2 dx \quad (22)$$

where  $\omega$  is given by equation 18. The definition of a positive frequency mode is that the mode have a definite frequency and that the inner product be positive, and thus that  $\pm F(k)$  be positive. This selects the positive sign for  $k > 0$  and the negative for  $k < 0$  and independent of the sign of  $\omega$ .

One can rephrase the above discussion by stating that one is defining positive frequency by the sign of the frequency in the co-moving frame. Defining  $x' = x - vt$ , the mode  $e^{i(\omega_p m t + kx)}$  becomes  $e^{i((\omega_p m - kv)t + kx')} = e^{i(\pm |F(k)| t + kx')}$ .

In the case of the usual black hole situation, or the case in which the dispersion relation is linear for all frequencies for the dumb hole, we must propagate the packet backward in time until it enters the region of black (or dumb) hole formation. During that back propagation, the packet is constantly blue shifting, so that the frequency of the wave by the time it reaches the formation time is absurdly high. This is clearly not calculable numerically, but the process has been well understood analytically since Hawking's original calculation. In the case in which the dispersion relation is such that  $\omega$  becomes a constant at high frequencies, however, the calculation can be done numerically, and the positive and negative frequency overlap integral can be computed numerically.

The dispersion function  $F$  is taken to be given by

$$F(k) = k_0 \tanh\left(\left(\frac{k}{k_0}\right)^n\right)^{\frac{1}{n}} \quad (23)$$

where  $k_0$  is the spatial frequency at which the dispersion function changes from linear to constant. This gives the length scale over which the dispersion function leads to a non-locality in the propagation equations of about  $2\pi/k_0$ . The parameter  $n$  determines the sharpness of the transition, with large  $n$  implying a very fast transition between the two regimes. I have studied what happens with  $n = 1$  and  $n = 4$  in most detail. A calculation with  $n = \infty$  was also carried out and the results were essentially the same as those for  $n = 4$ . I will first describe the  $n = 1$  case in some detail, and then briefly present the results for  $n = 4$ .

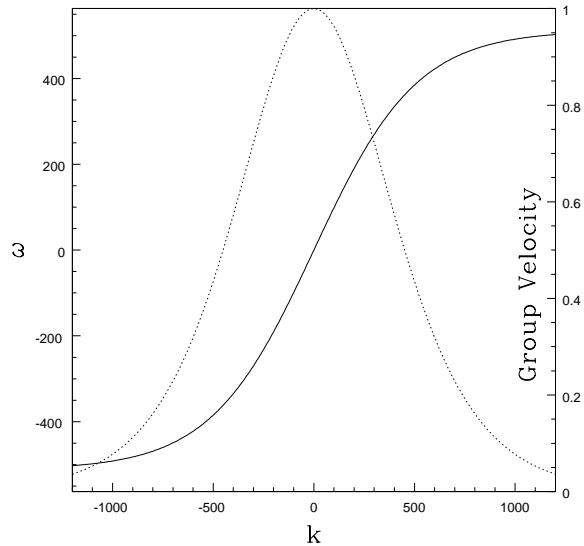


Figure 1

*The soft dispersion function ( $n = 1$ ) and corresponding group velocity (dotted line) at zero fluid velocity. The transition wave number  $k_0$  is 512.*

A non-linear dispersion function means that the group velocity of the wave when the fluid velocity,  $v$  is 0, namely

$$v_g = \frac{d\omega}{dk}, \quad (24)$$

is not a constant, but depends on frequency. In figure 1 is plotted  $\omega$  and  $v_g$ , the group velocity, as a functions of  $k$  for the value of  $n = 1$ . One can now give a hand waving description of the effect of this non-trivial dispersion function on the behaviour of a wave packet. I will describe ( and in the next section analyze) the problem by propagating an outgoing packet backward in time. Consider a long wavelength packet which is an outgoing packet at late times. It travels outward away from the sonic horizon and against the fluid flow. As we go backward in time, it approaches nearer and nearer the horizon, until when it is sufficiently close it begins to blue shift exponentially. Eventually the frequency becomes sufficiently high that the group velocity of the wave is less that the velocity of the fluid at the horizon. The fluid therefore drags this outgoing packet in toward the hole ( or, since we are examining the system backward in time, the packet at earlier times is further and further from the horizon). The packet seems to bounce off the horizon because of the change in the relation of the group and the fluid velocity of the packet.

The naive picture is however complicated by the fact that the blue shift of the wave near the horizon is spatially very non-uniform. The front edge of the wave, the edge nearest the horizon, is blue shifted to a much larger extent ( at any given time) than the trailing edge of the wave. In fact the leading edge is blue shifted to the final frequency long before the tail of the pulse has come near the sonic horizon. Thus, it seems dangerous to simply analyze the process either in position space, or in momentum space.

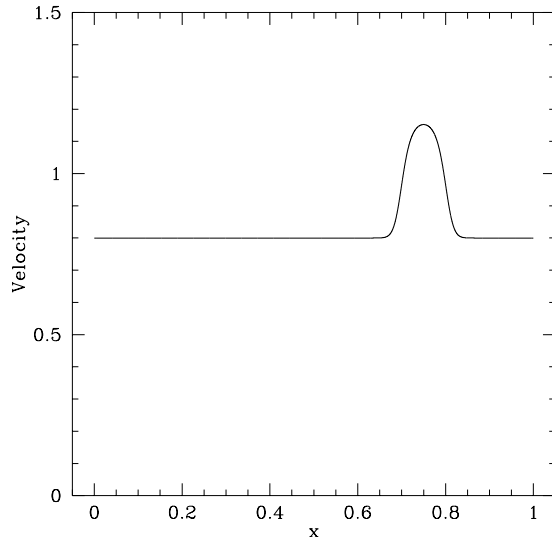


Figure 2

*The velocity profile of the fluid used. The system is assumed to have periodic boundary conditions. Note that  $x \approx .7$  corresponds to the horizon.  $x \approx .8$  is a Cauchy horizon.*

However, the numerical calculation seems to support this naive picture. In the numerical calculations, I have chosen my space to have periodic boundary conditions with  $x = 0$  identified with  $x = 1$ . This was done primarily because of the difficulty of specifying any other boundary conditions with the non-trivial wave equation with its unusual dispersion relations. The velocity field is chosen to be given by the function

$$v(x) = 1 - .2 \tanh(24 \cos(2\pi(x - .25)) + 23) \quad (25)$$

which is plotted in figure 2. This function, which is constant with value of .8 (in units where the low wave number velocity of sound in a still fluid is unity) over most of the range, was chosen precisely to have a broad range of constant value with a smooth transition to a region where  $v > 1$ . Although the region where  $v > 1$  is small, this turns out to be irrelevant because the wave never penetrates that region. The horizon occurs where  $v(x) = 1$ , which is where  $\cos(2\pi(x - .25)) = -23/24$ , or  $x \approx .75 \pm .046$ . It is the lower value ( $x \approx .7$ ) which represents the horizon, while the other represents an irrelevant Cauchy horizon.

Another value of interest is the derivative of velocity with respect to position,  $\frac{dv}{dx}$  at the horizon, since this gives the temperature. This is given by

$$\left. \frac{dv}{dx} \right|_{v=1} = .2(48\pi\sqrt{1 - (23/24)^2}) = .4\pi\sqrt{47} \approx 8.6 \quad (26)$$

giving a temperature of

$$T = \frac{1}{2\pi} \frac{dv}{dx} = 1.37. \quad (27)$$

(Recall that our units are such that  $v_g(k = 0) = 1$ , so that the thermal wave number is  $k_T \approx 1/T$  and the thermal wave length is thus approximately 8, which is longer than the whole spatial domain.

The final (late in time) wave packets (recall that we will be propagating the packets backward in time), chosen to be purely negative frequency packets, are thus complex, and are traveling away from the horizon. They are confined as much as is possible to the region where the velocity is constant. They now travel (backwards in time) toward the horizon of the dumb hole, where they begin to blue shift. Eventually their frequency becomes sufficiently high that the group velocity drops to less than unity and they are dragged backward out of the region of the hole to the region where the fluid velocity is constant. In this region we can again analyze the wave into its positive and negative frequency parts, and determine the Bogoliubov transformation quantity for this particular wave packet.

This analysis must be carried out in the constant velocity regions. Whether or not a wave is "positive frequency" depends on its time dependent behaviour. However, both because of the finite size of the system, and because of the finite time for which one can reliably carry out the integration, the temporal behaviour is difficult to use in determining whether or not the wave is positive frequency. However, in regions where the fluid velocity is constant, one can directly compare the relation between the field and its first time derivative to determine its positive and negative frequency components. We have

$$\begin{aligned}(\partial_t - v\partial_x)\phi &= \pi \\(\partial_t - v\partial_x)\pi &= F^2(\partial_x)\phi\end{aligned}\tag{28}$$

Fourier transforming under the assumption that  $v$  is a constant, we have

$$\begin{aligned}(\omega_{\pm} - vk)\tilde{\phi}_{\pm}(k) &= \tilde{\pi}_{\pm}(k) \\(\omega_{\pm} - vk)\tilde{\pi}_{\pm}(k) &= F^2(k)\tilde{\phi}_{\pm}(k)\end{aligned}\tag{29}$$

We can solve for  $\omega$  and choose that

$$\omega_{\pm} = vk \pm |F(k)|\tag{30}$$

with  $\omega_+$  the positive frequency branch for all values of  $k$  (independent of the sign of  $\omega_+$ ).

Now, given  $\tilde{\phi}(t, k)$  and  $\tilde{\pi}(t, k)$  we can split it into its positive and negative frequency parts by  $\tilde{\phi}(k) = \tilde{\phi}_+(k) + \tilde{\phi}_-(k)$  and  $\tilde{\pi}(k) = \tilde{\pi}_+(k) + \tilde{\pi}_-(k)$ , and the  $\pm$  subscript denotes the positive and negative frequency component. Solving for the positive frequency part, we get

$$\begin{aligned}\tilde{\phi}_+(k) &= \frac{1}{2}((-i\tilde{\pi}(k)/|F(k)| + \tilde{\phi}(k)) \\ \tilde{\pi}_+(k) &= \frac{1}{2}((\tilde{\pi}(k) - i|F(k)|\tilde{\phi}(k))\end{aligned}\tag{31}$$

The procedure now is to set up the initial (late time) wave as a purely negative frequency wave, propagate it backward in time until the resultant wave is again entirely (or as much as is possible) in the constant velocity regime. The resultant wave is then analyzed into its positive and negative frequency parts, and the inner product of each of these parts separately is calculated. Note that the inner product of the full wave itself is conserved, and this can be used as a test of the integration routine. We finally get the actual Bogoliubov coefficients for the wave from the future to the past (and thus also from the past to the future) and can compare this with the thermal hypothesis.

One can also calculate the expected Bogoliubov coefficient under the assumption that the outgoing mode is thermally distributed, as would be expected from the naive application of the Hawking procedure to the wave. The wave packets used are not plane wave states, and thus one must integrate the thermal factor over the spectrum of the outgoing wave to find the expected amplitude of the thermal Bogoliubov coefficient. If this thermal factor equals the Bogoliubov coefficient calculated from the evolution equations, then the thermal radiation for dumb holes hypothesis is validated even with this non standard high frequency dispersion function.

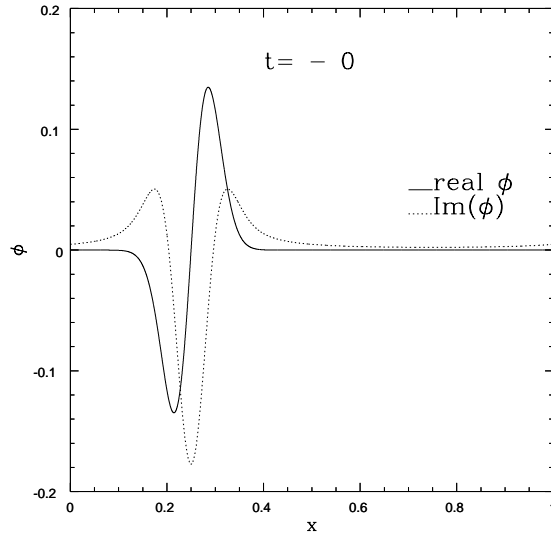


Figure 3

*The Real (solid line) and Imaginary (dotted line) parts of a final pulse emerging from the dumb hole. The dispersion function has  $n = 1$  and  $k_0 = 512$ .*

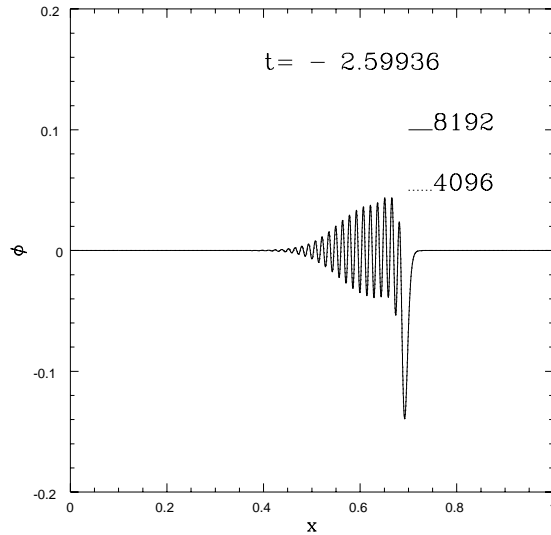


Figure 4

*An intermediate stage in the evolution backward in time of the real part of the pulse of figure 3. Note that the front of the wave has crashed into the horizon, and been blue shifted to a*

high frequency pulse whose group velocity is less than the fluid velocity. The dotted line is the same calculation but at half the spatial resolution as the solid line.

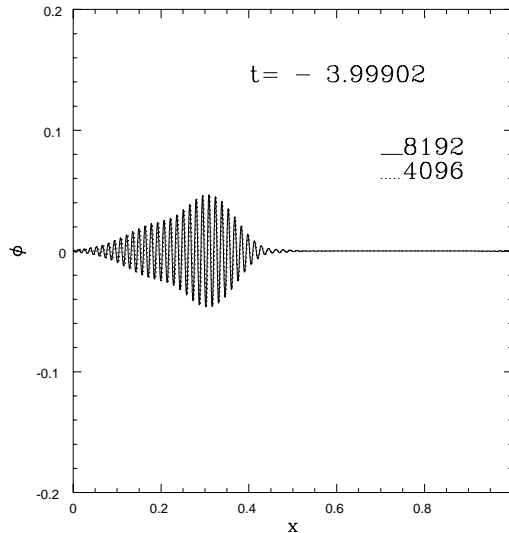


Figure 5

The pulse as it must have been initially to produce the outgoing pulse of figure 3. Note that it is an outgoing pulse but is being dragged in toward the horizon by the inflowing fluid. Again the dotted line is at half the resolution as the solid line to give an estimate of the numerical errors.

Figures 3 gives the real (solid line) and imaginary (dotted line) parts of the wave packet at the final time. In figures 4 and 5 I show the real part of the wave at two separate earlier times. In figure 4 the wave is just interacting with the horizon. Part of the wave has been blue shifted (going backwards in time) and part is still at the final low frequency. Figure 6 gives the incoming wave in the constant velocity region as it must have been in order to produce the outgoing wave of figure 3. We note in figure 4 that the front edge of the wave has already crashed into the “horizon” ( $v = 1$ ), been blue-shifted and begun to be dragged back out of the dumb hole by the inflowing (which in the reverse time direction is outflowing) fluid because its group velocity has decreased at the higher frequencies. At the same time the trailing edge of the pulse is still traveling toward the hole.

In figures 4 and 5 I also show the outcome of the numerical evolution for two different grid spacings (the dotted is at half the resolution of the solid line) to give a feeling for the accuracy of the integration. The key difference is in the phase velocity of the wave being dragged out of the hole. This is expected, because of the finite differencing of the term  $v\partial_x$  term in the equations. The centered differencing scheme converts this term to  $iv \sin(2k\Delta_x)/2\Delta_x$  instead of the exact  $ivk$ . This means that at large  $k$ , the effective velocity of the fluid is decreased by  $\sin(2k\Delta_x)/2k\Delta_x$ . I.e., at high frequencies, the effective fluid velocity is less leading to a slightly smaller dragging velocity for the high frequency wave, as is seen in the simulation.

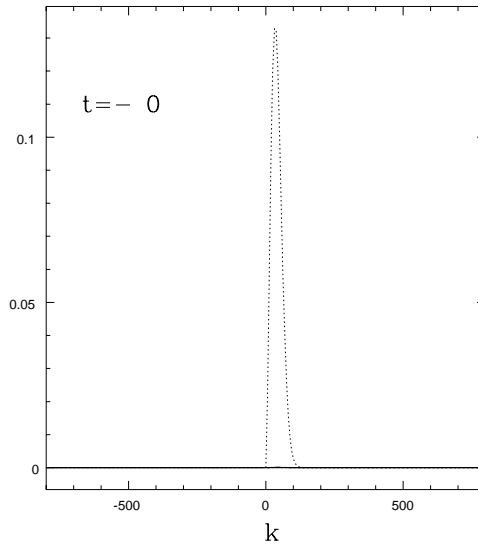


Figure 6

*The spectrum of the final pulse of figure 3. Note that it is purely positive wave number and negative frequency.*

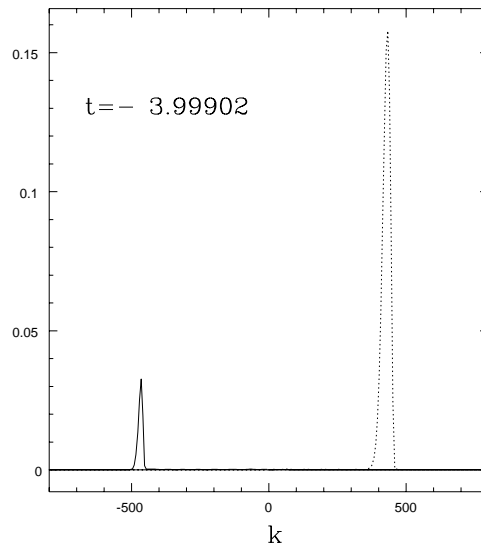


Figure 7

*The spectrum of the initial pulse of figure 5. The solid line is positive frequency components while the dotted line is negative frequencies. Since positive frequencies correspond to positive wave number and vice versa, this still represents a purely outgoing wave.*

In figure 6 I give the spectrum ( in  $k$  space) of the final outgoing wave packet. This wave has been designed to be purely negative frequency, left traveling and concentrated in the region where the velocity is constant. It represents a wave packet traveling away from the hole against the inflowing fluid flow. In figure 7 we have the spectrum corresponding to figure 6 , divided into positive and negative frequency parts, again in  $k$  space. The dotted line is the negative frequency components while the solid line represents the positive frequency components. We note that to very good accuracy, the interaction with the horizon

has left the wave as a wave purely traveling to the left ( even though the fluid velocity is now sufficiently high to drag the left traveling wave to the right). The positive  $k$  modes are negative frequency while the negative  $k$  modes are positive frequency.

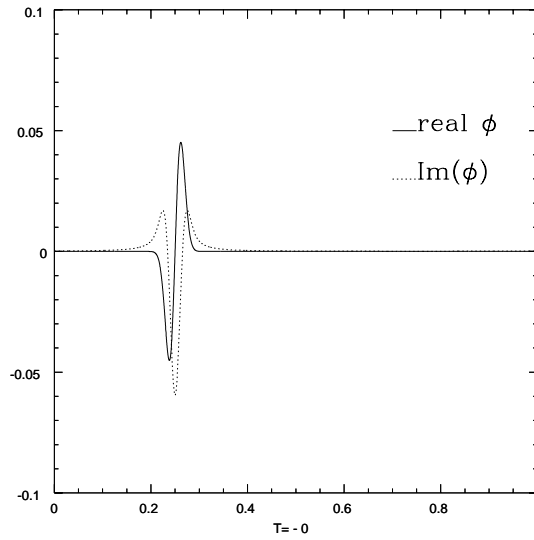


Figure 8

*A narrower final pulse but otherwise the same as in Figure 3.*

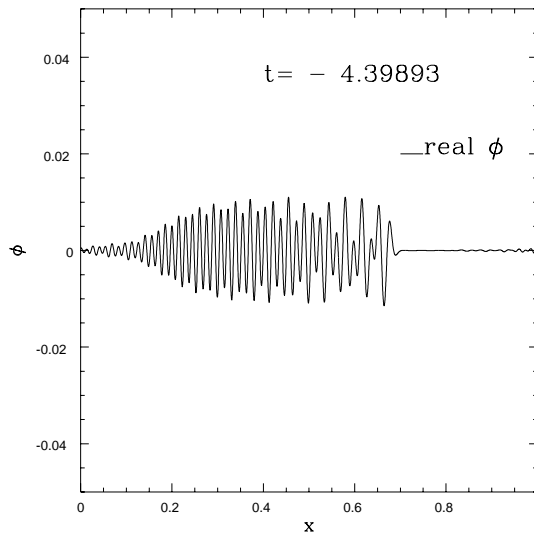


Figure 9

*The initial pulse which must have produced figure 8.*

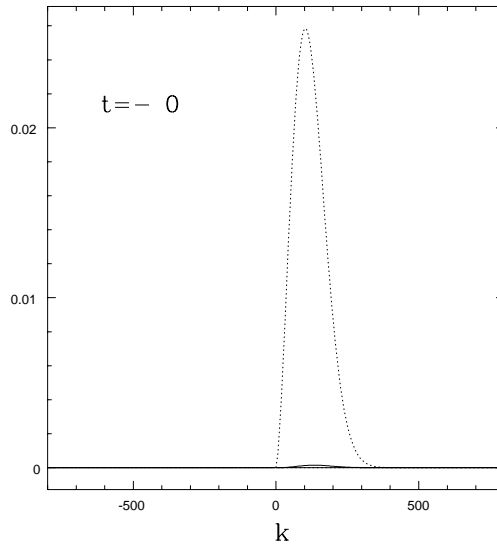


Figure 10

*The spectrum of the final pulse of figure 8.*

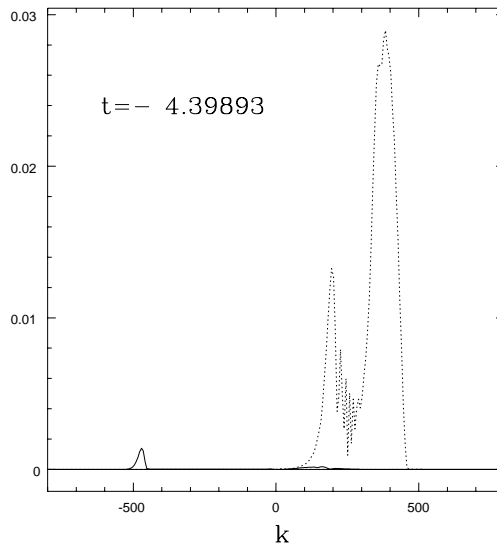


Figure 11

*The positive and negative frequency spectrum corresponding to figure 9. Note the much smaller positive frequency components than in Figure 7. Note that the power which has not been blue shifted corresponds to components of the initial packet whose group velocity was already of the order of or less than .8, the minimum velocity of the fluid.*

Figures 8 and 9 give the final and initial wave packets for another higher frequency pulse while figures 10 and 11 give the spectra of these pulses again split into positive and negative frequency parts. We see in figure 11 a much smaller conversion of positive to negative frequency, as would have been expected from the higher frequency of the initial pulse. All of these cases are for the  $n = 1$  dispersion function.

Let us now compare the above with the value for the total Bogoliubov transformation expected on the thermal hypothesis.

Given the final mode represented by figure 3 or 8, the expected number of particles resident in this mode in a thermal state of temperature  $T$  is given by

$$\beta_T = \frac{1}{\mathcal{N}} \int \frac{e^{-\omega T}}{1 - e^{-\omega T}} \left( \tilde{\pi}^*(k) \tilde{\phi}(k) - \tilde{\phi}^*(k) \pi(k) \right) dk \quad (32)$$

where  $\mathcal{N}$  is the normalization factor

$$\mathcal{N} = \int \left( \tilde{\pi}^*(k) \tilde{\phi}(k) - \tilde{\phi}^*(k) \pi(k) \right) dk \quad (33)$$

On the other hand, the expected number of particles in this mode,  $\beta$ , if we assume that the input state was in the vacuum state is just given by the positive frequency portion of the initial wave form ( the Bogoliubov coefficient). This is just the norm of the positive frequency part of the normalized wave.

Comparing the two values, we find for the low frequency pulse in the soft ( $n = 1$ ) dispersion function case that

$$\beta_T = .02302; \quad \beta = .02336 \quad (34)$$

while for the high frequency pulse

$$\beta_T = .0005364; \quad \beta = .0005545 \quad (35)$$

In each case the Bogoliubov estimate of the particle production in that particular pulse is essentially the same as the thermal estimate. The change in high frequency behaviour of the theory makes little or no difference to the expected thermal output from the dumb hole. ( I suspect the error to be related to the fact that the final wave pulse is not entirely contained within the constant velocity region.)

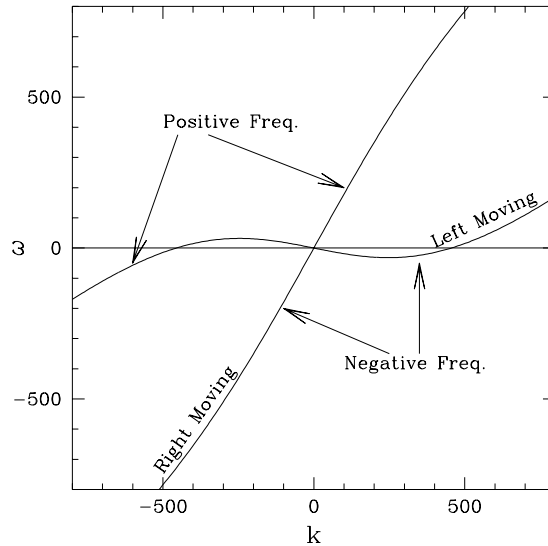


Figure 12

*The relation between  $\omega$ , the temporal frequency, and  $k$  the wave number in the constant velocity ( $V = .8$ ) region . The various branches (positive and negative frequency and right and left moving) of the dispersion relation are labeled.*

Moreover, in addition to the integrated Bogoliubov transformation, one can test whether the full spectrum itself of the outgoing radiation is thermal. Since the velocity in the simulation is time independent, the frequency of any wave in the continuum, infinite spatial section case is conserved. Consider an final left moving pulse, contained entirely in the constant velocity region, with components  $\tilde{\phi}(k)$ . For any value of  $k$ , there are two possible values for the frequency  $\omega$  as given in figure 12. Since the pulses are left moving pulses, the relation between the frequency  $\omega$  and  $k$  is given by the left-moving branch labeled as such in the figure. Since the final pulse is chosen to be a purely negative frequency pulse, it is, as mentioned previously, composed of purely positive values of  $k$ . Now evolve the wave backward in time until one has evolved it past its interaction with the horizon and back out into the region where the velocity is a constant. Because the problem is time independent, the frequency  $\omega$  is conserved. Thus the amplitude of the wave over some finite frequency regime must be the same. Furthermore, we have already noted that the left moving wave remains a left moving wave, and thus remains on the same left moving branch of the dispersion relation.

This amplitude is given by

$$\int \tilde{\pi}^*(t, k) \tilde{\phi}(t, k) dk \quad (36)$$

However, on the left moving branch, we have a definite relation between  $\omega$  and  $k$ , and between  $\tilde{\pi}(t, k)$  and  $\tilde{\phi}(t, k)$ . In particular for the left moving branch,  $\tilde{\pi}(t, k) = +F(k)\tilde{\phi}(t, k)$ . Thus, we have that the magnitude of the wave over a frequency interval  $d\omega$  is

$$\int F(k) |\phi(t, k)|^2 \frac{dk}{d\omega} d\omega \quad (37)$$

where the integral is over all values of  $k$  for which  $\omega(k)$  has the desired value. From the plot we see that along the left moving branch there are three values of  $k$  for any value of  $\omega$  near zero. If we choose our initial pulse to have  $k$  positive, two of these lie on the negative frequency branch, and one lies on the positive frequency branch. Now the initial pulse is chosen to be non-zero only for small values of  $k$ . After the interaction with the horizon, the pulse has been blue shifted, and has non-zero values for  $k$  lying near  $\pm k_c$ , the wave number where the phase velocity of the waves in the constant velocity regions ( $\omega(k)/k$ ) is zero.

Let us define the three values of  $k$  at which the value of  $\omega$  is the same as  $k_i$ , for the value of  $k$  nearest  $k = 0$ ,  $k_n$  for the nearest value of  $k$  to  $+k_c$  and  $k_p = -k_n$  for the value nearest  $-k_c$ . Under the thermal hypothesis, the initial pulses, obtained by transporting the final pulse backward in time, will be composed of positive and negative frequency components, with the two magnitudes in a frequency interval related by

$$|F(k_p)\tilde{\phi}(k_p)^2/v_g(k_p)| = e^{-\omega(k_i)/T} |F(k_n)\tilde{\phi}(k_n)^2/v_g(k_n)| \quad (38)$$

where  $v_g(k) = \frac{d\omega(k)}{dk}$  is the group velocity at wave vector  $k$ . Furthermore, we should have

$$|F(k_p)\tilde{\phi}(k_p)^2/v_g(k_p)| = \frac{e^{-\omega(k_p)/T}}{1 - e^{-\omega(k_p)/T}} |F(k_i)\tilde{\phi}(k_i)^2/v_g(k_i)| \quad (39)$$

Only if these relations hold will the Bogoliubov transformation satisfy the thermal hypothesis for all final wave forms.

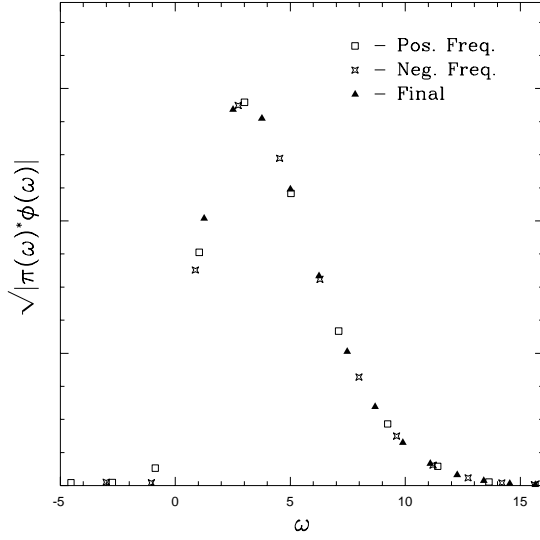


Figure 13

*The comparison between the thermal predictions for the positive frequency component of the outgoing pulse and the actual positive frequency component of the outgoing pulse.*

In figure 13 I have plotted the three functions  $|F(k_p)\hat{\phi}_i^+(k_p)^2/v_g(k_p)|^{1/2}$ , the positive frequency part of the initial pulse,  $|\frac{e^{-\omega(k_p)/T}}{1-e^{-\omega(k_p)/T}}F(k_i)\hat{\phi}_f(k_i)^2/v_g(k_i)|^{1/2}$ , the predicted positive frequency part of the initial pulse from the final pulse and  $|e^{-\omega(k_i)/T}F(k_n)\hat{\phi}_i^-(k_n)^2/v_g(k_n)|^{1/2}$ , the prediction of the positive frequency part of the final pulse from the negative frequency part of the final pulse. These are plotted against the frequency  $\omega$ . These are for the final pulse of figure 3 and associated initial pulse of figure 6. Note that if the first two agree, the last one's agreeing is a test of the conservation of the norm by the evolution. Because of the finite size of the region and the periodic boundary conditions, only a finite number of  $k$  values are calculated, but it is clear that these three curves are identical to numerical accuracy. Note that the temperature is of order 1.3, and this graph thus represents about 10 e-foldings of the thermal function. Thus we can conclude that not only are the two particular final wave forms chosen for the soft dispersion relation thermal, but that any final wave form would be thermal. Thus despite the change in the high frequency dispersion function, the output of the dumb hole will continue to be thermal. The spectrum, and not just the integrated intensity, is a thermal spectrum.

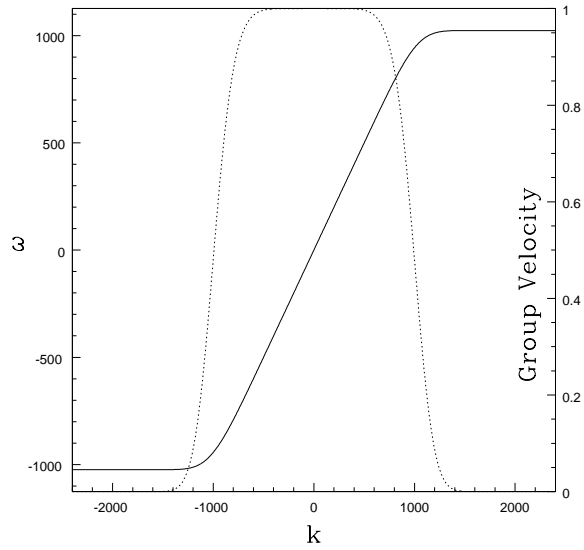


Figure 14

*The sharp dispersion function ( $n = 4$ ) and group velocity (dotted line) at zero fluid velocity. The transition wave number here is taken to be 1024.*

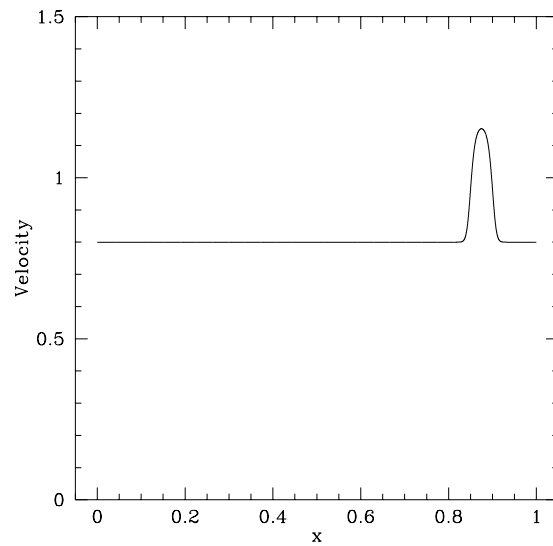


Figure 15

*The velocity profile for the sharp dispersion function. It is scaled by a factor of 2 from that of figure 1 to allow more room for the constant velocity region*

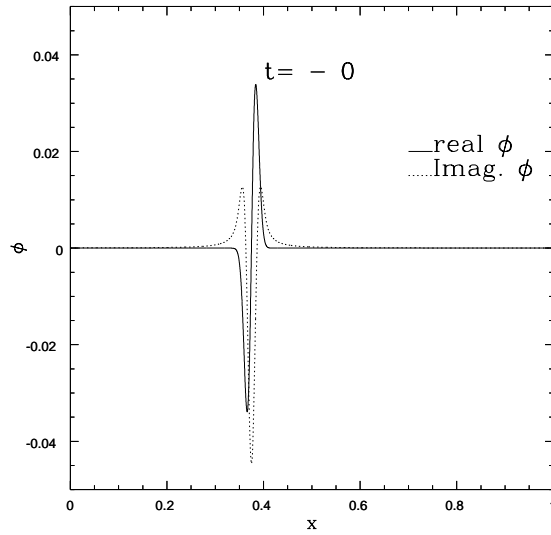


Figure 16

*The final pulse for the sharp dispersion function— it is scaled by a factor of 2 from figure 3*

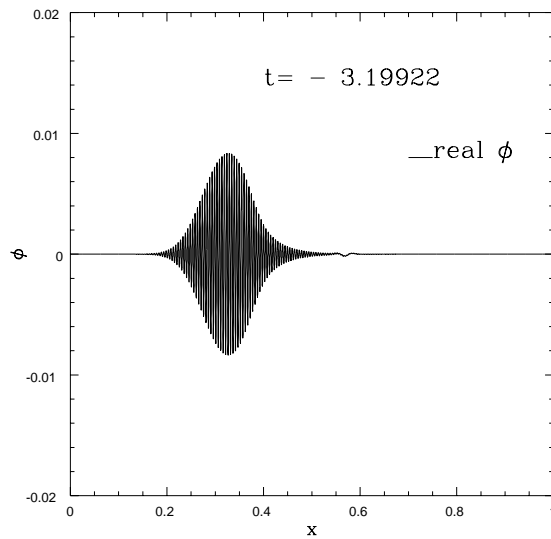


Figure 17

*The initial pulse which would have produced the final pulse of figure 4 rescaled by a factor of 1.5. Note that the initial pulse is more monochromatic than that of figure 6 because of the much sharper dispersion function.*

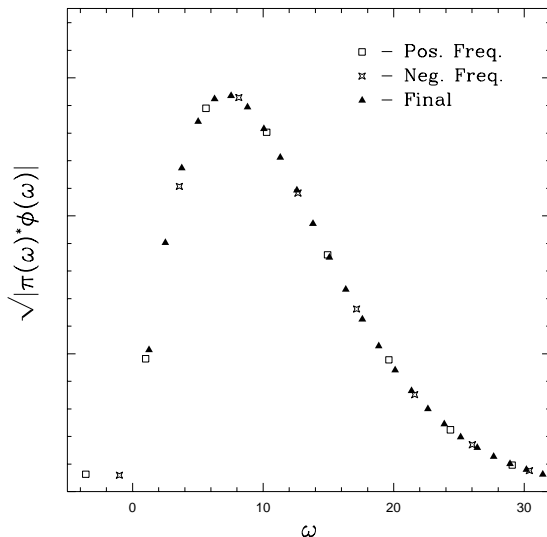


Figure 18

*The intensity of the positive frequency component of the initial pulse of fig. 15 together with the thermally scaled negative frequency spectrum of figure 16 and that of the final pulse of figure 3 (rescaled). Note that the thermal hypothesis does accurately predict the relations between the various components of the spectrum of the ingoing and outgoing pulses.*

The dispersion function with  $n = 1$  present a relatively gentle transition from the low frequency linear regime to the high frequency constant regime. If we alter the dispersion function to give a much more sudden transition, namely the dispersion function with  $n = 4$  (see fig. 14), does this alter the thermal spectrum of the emitted radiation? The answer is no. The sharp dispersion function has a much longer initial pulse for the same situation as used above for the  $n = 1$  case. In order to allow the initial pulse to be contained entirely within the constant velocity region, I have scaled the problem by a factor of 2. Thus the transition  $k_0$  in figure 14 is larger by 2 to 1024, the velocity profile of figure 15 has been rescaled by a factor of 2, increasing the temperature to approximately 2.7. The final pulse of figure 16 is just figure 3 rescaled by a factor of 2. In figure 17 I present the initial pulse which must have produced the final pulse of figure 16 in the case in which  $n = 4$ . Despite the far more sudden transition between the regimes in the dispersion function, the relation between the final and the initial pulses is again accurately given by a thermal relation as plotted in figure 18. Again the final positive and negative frequency components of the initial pulse can be accurately predicted from the final pulse using the thermal hypothesis.

### III. DISCUSSION

Why are the results thermal, and what lessons can we learn from this simple problem for the more interesting one of black hole evaporation? The crucial lessons seems to be that, despite the naive derivations, black hole evaporation depends neither on the ultra high frequency behaviour of the fields near the black hole, nor on the behaviour of the field theory in imaginary time. The process of the thermal particle creation appears to be primarily a low, not high, energy phenomenon. The black hole and dumb hole have

natural time scales- the the mass in the former case, and the inverse gradient of velocity in the latter. The behaviour of the fields near the horizon of the holes is governed by these relatively (compared with Plank or atomic) time scales. In the vicinity of the hole, the fields experience changes on these scales. However, as far as the high frequency parts of the field are concerned, these time scales are very long and the changes are slow. The high frequency phenomena simply adjust adiabatically to these slow changes. If the state is the vacuum state at high frequencies, it remains the vacuum. One would expect this to remain true no matter what the form of the theory was at those high frequencies and energies. It is only in the regime where the natural time scale of the hole is of the same order as the time scale of the field theory that these slow changes near the hole can make their influence felt. I.e., it is only for those wave whose frequencies are of the order of  $1/M$  for the black hole that anything happens.

On that time scale, the structure near the black hole is that the null geodesics diverge exponentially. The time between neighbouring outgoing geodesics is exponential in the affine parameter along the geodesics. It is this exponential divergence ( shared by both the black hole and the dumb hole) that leads to the thermal spectrum emitted by the hole. It is this exponential divergence at the low frequency time scale, and not at the highest frequencies of the theory that matters for the thermal emission.

One can encapsulate this freedom of the low frequency thermal emission from traces of the high frequency behaviour of the theory by the phrase that dumb holes (and thus by hypothesis also black holes) have no quantum hair. Just as the red shift at the horizon wipes out all traces of the rich complexity of classical material which could have formed the black hole, it also seems to wipe out all traces of the quantum structures at high frequencies wich are red shifted to form the thermal radiation from the black hole.

## ACKNOWLEDGMENTS

I would like to thank Ted Jacobson who revived my interest in dumb holes, and pointed out in conversations and in ref. [3] that one of the crucial effects of the atomic nature of matter is to alter the high frequency dispersion relation of the sound waves. Conversations with him have been very helpful to me in understanding dumb holes. I would also like to thank Matt Choptuik who insisted through the years on thinking about the stability of the solution scheme before coding rather than when the numerical instabilities become obvious. Without the lessons he taught me I would not have solved this problem. In addition a conversation with him on the numerical techniques needed for this problem gave me the courage to attack it. This research was carried out under a Fellowship from the Canadian Institute for Advanced Research and with an NSERC research grant.

## APPENDIX A: NUMERICAL TECHNIQUE

The equations of motion for the system are solved via a set of implicit, symmetric in space and time, finite difference equations. The spatial grid  $\{x_i\}$  is taken as a uniform grid, with  $\Delta_x \equiv x_{i+1} - x_i$ . The term  $[F(\partial_x^2)\phi](x_i)$  is evaluated by taking the FFT of  $\phi(x_i)$ ,  $\tilde{\phi}(k_j)$ , multiplying by  $F(-k_j^2)$ , and then taking the inverse FFT. The temporal grid is staggered,

with  $\phi_{m,i} = \phi(t_m, x_i)$  defined on the time slices  $t_i$  with uniform differences  $\Delta_t = t_{m+1} - t_m$ . The  $\pi$  on the other hand are evaluated on the staggered sites  $\pi_{m,i} = \pi(t_m + \frac{1}{2}\Delta_t, x_j)$ . The grid points run from 0 to  $N + 1$  where  $N = 1/\Delta_x$ . The periodic boundary conditions are enforced by taking  $\phi_{m,N} = \phi_{m,0}$  and  $\phi_{m,N+1} = \phi_{m,1}$ , and similarly for  $\pi$ .

The differencing step equations are taken to be

$$\begin{aligned} \phi_{m+1,i} - \frac{\Delta_t}{2\Delta_x} (v(x_{i+1}\phi_{m+1,i+1} - v(x_{i-1}\phi_{m+1,i-1})) \\ = \phi_{m,i} + \frac{\Delta_t}{2\Delta_x} (v(x_{i+1}\phi_{m,i+1} - v(x_{i-1}\phi_{m,i-1})) + \Delta_t\pi_{m,i} \end{aligned} \quad (\text{A1})$$

$$\begin{aligned} \pi_{m+1,i} - \frac{\Delta_t}{2\Delta_x} v(x_i) (\pi_{m+1,i+1} - \pi_{m+1,i-1}) \\ = \phi_{m,i} + \frac{\Delta_t}{2\Delta_x} v(x_i) (\pi_{m,i+1} - \pi_{m,i-1}) + \Delta_t[F(\partial_x^2)\phi]_{m+1,i} \end{aligned} \quad (\text{A2})$$

This differencing technique was chosen because, if we take  $v$  as a constant, these equations can be shown to be stable, and non-damping. Both of these characteristics are crucial for the success of the integration. The stability is important because of the severe frequency shifting that takes place on the horizon, a frequency shifting which could easily incite any instabilities present in the code. The non-damping nature is also crucial because of the necessity of extracting small effects ( the Bogoliubov coefficients) from the result of the evolution. In particular, since we are testing precisely the high frequency effects, it is important not to hide these behind artificial viscosity at high frequencies.

To see the stability, assume that the velocity is constant, and Fourier analyze the difference equations in both space and time. We get the characteristic equation

$$(2i \sin(\omega\Delta_t/2) - iv\frac{\Delta_t}{\Delta_x} \sin(k\Delta_x))^2 = \Delta_t^2 F(-k^2) \quad (\text{A3})$$

or

$$\sin(\omega\Delta_t/2) = \frac{1}{2}\Delta_t \left( \pm\sqrt{-F(-k^2)} + \frac{v}{\Delta_x} \sin(2k\Delta_x) \right) \quad (\text{A4})$$

This will have real solutions for  $\omega$  for all  $k$  as long as  $\frac{\Delta_t}{\Delta_x}$  is chosen to be sufficiently small. In particular the RHS of the equation must be less than unity for all values of  $k$ . Since  $-F(-k^2)$  is bounded by  $k_0^2$ , and  $k_0 < k_{max} = \frac{\pi}{\Delta_x}$ , and since  $\sin(2k\Delta_x) < 1$ , the right hand side is bounded by  $\Delta_t \left( k_0 + \frac{v}{\Delta_x} \right)$  so we require

$$\Delta_t < \frac{\Delta_x}{k_0\Delta_x + v_{max}} \quad (\text{A5})$$

in which case the  $\omega$  are all real— the equations are stable, and non-damping. This would not have been true had I employed an explicit scheme for the time difference equations.

Because of the use of an implicit scheme, the time stepping requires the inversion of matrix equation. To solve this, I used a double sweep technique. To illustrate the technique, let us solve the equation

$$V_i^0 U_i - V_i^p U_{i+1} + V_i^n U_{i-1} = S_i \quad (\text{A6})$$

Both of the equations for the time stepping are of this form, with different coefficient vectors  $V^0, V^n, V^p$ . These coefficients are the same at all times as they depend only on  $v$  and  $\frac{\Delta t}{\Delta x}$ . The solution will be found by assuming the recursion relation

$$U_i = A_i U_{i-1} + B_i \quad (\text{A7})$$

First solve the recursion relation by substituting for  $U_{i+1}$  and  $U_i$  using this recursion relation into eqn A6. Setting the coefficients of  $U_{i-1}$  to zero, we get recursion relations for the  $A_i$  and  $B_i$ :

$$A_i = -\frac{V_i^n}{A_{i+1}V_i^p + V_i^0} \quad (\text{A8})$$

$$B_i = -\frac{V_i^p B_{i+1}}{A_{i+1}V_i^p + V_i^0} \quad (\text{A9})$$

with  $B_{N+1} = 1$ . Now find two solutions to the homogeneous equations

$$U_{i+1}^0 = A_{i+1}U_i^0 + B_i \quad (\text{A10})$$

$$U_{i+1}^1 = A_{i+1}U_i^1 \quad (\text{A11})$$

with  $U_0^0 = 0$  and  $U_0^1 = 1$ . Neither of these are periodic.

To find a periodic solution to the non-homogeneous equations, first recursively solve

$$B_i = \frac{S_i - V_i^p B_{i+1}}{A_{i+1}V_i^p + V_i^0} \quad (\text{A12})$$

with  $B_{N+1} = 0$ . Then recursively solve

$$U_i = A_i U_{i-1} + B_i \quad (\text{A13})$$

with  $U_0 = 0$  This will not satisfy the boundary conditions. However, one can now subtract a suitable linear combination of  $U^0$  and  $U^1$  to enforce the periodic boundary conditions.

## REFERENCES

- [1] Comm Math Phys **43** 199 (1975)
- [2] W.G. Unruh Phys Rev Lett **46** 1351 (1981)
- [3] T. Jacobson Phys Rev **D44** 1731 (1991)
- [4] G. Gibbons, S.W. Hawking Phys Rev **D** 2752(1977)

## FIGURES

FIG. 1. The soft dispersion function ( $n = 1$ ) and corresponding group velocity (dotted line) at zero fluid velocity. The transition wave number  $k_0$  is 512.

FIG. 2. The velocity profile of the fluid used. The system is assumed to have periodic boundary conditions. Note that  $x \approx .7$  corresponds to the horizon.  $x \approx .8$  is a Cauchy horizon.

FIG. 3. The Real (solid line) and Imaginary (dotted line) parts of a final pulse emerging from the dumb hole. The dispersion function has  $n = 1$  and  $k_0 = 512$ .

FIG. 4. An intermediate stage in the evolution backward in time of the real part of the pulse of figure 3. Note that the front of the wave has crashed into the horizon, and been blue shifted to a high frequency pulse whose group velocity is less than the fluid velocity. The dotted line is the same calculation but at half the spatial resolution as the solid line.

FIG. 5. The pulse as it must have been initially to produce the outgoing pulse of figure 3. Note that it is an outgoing pulse but is being dragged in toward the horizon by the inflowing fluid. Again the dotted line is at half the resolution as the solid line to give an estimate of the numerical errors.

FIG. 6. The spectrum of the final pulse of figure 3. Note that it is purely positive wave number and negative frequency.

FIG. 7. The spectrum of the initial pulse of figure 5. The solid line is positive frequency components while the dotted line is negative frequencies. Since positive frequencies correspond to positive wave number and vice versa, this still represents a purely outgoing wave.

FIG. 8. A narrower final pulse but otherwise the same as in Figure 3.

FIG. 9. The initial pulse which must have produced figure 8.

FIG. 10. The spectrum of the final pulse of figure 8.

FIG. 11. The positive and negative frequency spectrum corresponding to figure 9. Note the much smaller positive frequency components than in Figure 7. Note that the power which has not been blue shifted corresponds to components of the initial packet whose group velocity was already of the order of or less than .8, the minimum velocity of the fluid.

FIG. 12. The relation between  $\omega$ , the temporal frequency, and  $k$  the wave number in the constant velocity ( $V = .8$ ) region. The various branches (positive and negative frequency and right and left moving) of the dispersion relation are labeled.

FIG. 13. The comparison between the thermal predictions for the positive frequency component of the outgoing pulse and the actual positive frequency component of the outgoing pulse.

FIG. 14. The sharp dispersion function ( $n = 4$ ) and group velocity (dotted line) at zero fluid velocity. The transition wave number here is taken to be 1024.

FIG. 15. The velocity profile for the sharp dispersion function. It is scaled by a factor of 2 from that of figure 1 to allow more room for the constant velocity region

FIG. 16. The final pulse for the sharp dispersion function— it is scaled by a factor of 2 from fig. 3

FIG. 17. The initial pulse which would have produced the final pulse of figure 16.

FIG. 18. The intensity of the positive frequency component of the initial pulse of fig. 15 together with the thermally scaled negative frequency spectrum of figure 16 and that of the final pulse of figure 3 (rescaled). Note that the thermal hypothesis does accurately predict the relations between the various components of the spectrum of the ingoing and outgoing pulses.